
MOX-Report No. 63/2020

# HEMODYNAMICS AND REMODELING OF THE PORTAL CONFLUENCE IN PATIENTS WITH CANCER OF THE PANCREATIC HEAD: A PILOT STUDY

Tuveri, M.; Milani, E.; Marchegiani, G.; Landoni, L.; Torresani, E.; Capelli, P.; Sperandio, N.; D'Onofrio, M.; Salvia, R.; Vergara, C.; Bassi, C.

MOX, Dipartimento di Matematica
Politecnico di Milano, Via Bonardi 9 - 20133 Milano (Italy)

mox-dmat@polimi.it http://mox.polimi.it

# HEMODYNAMICS AND REMODELING OF THE PORTAL CONFLUENCE IN PATIENTS WITH CANCER OF THE PANCREATIC HEAD: A PILOT STUDY

M. Tuveri[1], E. Milani[2], G. Marchegiani[1], L. Landoni[1], E. Torresani[3], P. Capelli[3], N. Sperandio[4], M. D'Onofrio[5], R. Salvia[1], C. Vergara[6], C. Bassi[1]

1. Massimiliano Tuveri, MD, General and Pancreatic Surgery Unit, Pancreas Institute, University of Verona, Verona, Italy; massimiliano.tuveri@aovr.veneto.it
2. Eleonora Milani, MOX, Dipartimento di Matematica, Politecnico di Milano, Milano, Italy; eleonora.milani@mail.polimi.it
1. Luca Landoni, MD, General and Pancreatic Surgery Unit, Pancreas Institute, University of Verona, Verona, Italy; luca.landoni@aovr.veneto.it
1. Giovanni Marchegiani, MD, PhD, General and Pancreatic Surgery Unit, Pancreas Institute, University of Verona, Verona, Italy; giovanni.marchegiani@aovr.veneto.it
3. Evelin Torresani, Section of Pathology, Department of Diagnostics and Public Health, Pancreas Institute, University of Verona, Verona, Italy; evelintorresani@hotmail.it
3. Paola Capelli, Section of Pathology, Department of Diagnostics and Public Health, Pancreas Institute, University of Verona, Verona, Italy; paola.capelli@aovr.veneto.it
4. Nicola Sperandio, MLT, ARC-Net Research Center, University of Verona, Verona, Italy; nicola.sperandio@univr.it
5. Mirko D'Onofrio, MD, Department of Radiology, Pancreas Institute, University of Verona, Verona, Italy; mirko.donofrio@univr.it
1. Roberto Salvia, MD, PhD, General and Pancreatic Surgery Unit, Pancreas Institute, University of Verona, Verona, Italy; roberto.salvia@univr.it
6. Christian Vergara, LABS, Dipartimento di Chimica, Materiali e Ingegneria Chimica, Politecnico di Milano, Milano, Italy; christian.vergara@polimi.it1. Claudio Bassi, MD, FACS, FRCS, General and Pancreatic Surgery Unit, Pancreas Institute, University of Verona, Verona, Italy; claudio.bassi@univr.it
1. Claudio Bassi, MD, FACS, FRCS, General and Pancreatic Surgery Unit, Pancreas Institute, University of Verona, Verona, Italy; claudio.bassi@univr.it

**Corresponding Author**
Prof. Claudio Bassi, MD, FACS, FRCS
General and Pancreatic Surgery Unit, Pancreas Institute,
University of Verona,
P.le L.A. Scuro n° 10, 37134 Verona;
phone number 045.8124553, fax number 045.8126895;
email: claudio.bassi@univr.it

## ARTICLE SUMMARY

We designed a computational study to evaluate the effects of hemodynamics on portal confluence remodeling in cancer of the pancreatic head. The importance of this study is the finding that altered flow conditions due to tumor growth can disrupt the balance between eutrophic remodeling and degradative process of the vein wall, leading to the complete substitution of the three-layered vein wall and the opportunity to perform a total pancreatectomy with en-bloc resection of the portal confluence.

**ABSTRACT**

**Background.** We designed a computational study to evaluate the effects of hemodynamics on portal confluence remodeling in real models of patients with cancer of the pancreatic head.

**Methods.** Patient-specific models were created according to enhanced computed tomography data. Fluid dynamics was simulated by using finite-element methods. Computational results were compared to morphological findings.

**Results.** Five patients underwent total pancreatectomy, one had duodenopancreatectomy. Portal confluence or superior mesenteric vein resection was performed en-bloc with the specimen. The comparison of hemodynamic results to histopathological findings showed that in patients without a critical stenosis and normal wall shear stress (WSS), the three-layered wall of the vessel was preserved and modifications of the vessel wall were only local and minimal, due to tumor infiltration. In patients with a critical stenosis and increased WSS the three-layered structure of the resected vein was widely modified and replaced by a dense inflammatory infiltrate with subintimal migration of smooth muscle cells (SMC), in absence of tumor infiltration.

**Conclusions**. The portal confluence involved by cancer undergoes a remodelling that is not only due to a wall infiltration by the tumor but also to persistent pathological levels of WSS that disrupt the balance between eutrophic remodeling and degradative process of the vein wall, with an almost complete derangement of the three-layered wall due to subintimal SMC migration and fibrosis.This finding compels surgeons to conceive a different approach to stenoses of the portal confluence, avoiding if possible any dissection of the pancreatic neck in order to prevent injuries to a fragile vein.

## INTRODUCTION

Portal district is often involved in cases of primitive and metastatic cancer of the pancreatic head[1]. Tumor invasion of the portal confluence by PDAC is common due to the anatomic proximity of the head of the pancreas and the surrounding veins. This involvement can vary from a solid soft-tissue contact with focal vessel narrowing to complete occlusion[2]. In these cases, known as borderline resectable (BR) or locally advanced (LA) disease, depending on the degree of vein involvement, anatomy can be severely modified making radical resection and vascular repair very difficult or impossibile[3]. Fortunately, in many cases this involvement is not a true venous invasion but just a tumor adhesion due to tumor-associated desmoplasia, radio-chemotherapy-induced fibrosis or fibrosis due to tumor regression[4,5]. From one hand neoadjuvant chemotherapy (NCT) can play an important role as induction strategy to reduce vascular involvement in order to improve future resectability[6], from the other hand further tumor growth or radio-chemotherapy-induced regression of the tumor can determine such a parenchymal rearrangement that can worsen the vein geometry leading to a loss of its biomechanical properties, making thus surgery hazardous[7].

Modifications of the vessel geometry and wall infiltration by tumors of the pancreatic head usually determine a modification of local hemodynamics that triggers a process known as vascular remodelling[8-10]. Vascular remodeling is in fact the process of adaptation of vessels in response to disease, injury or aging[11,12]. More exactly vessel remodeling is thought to reflect adaptation of the vessel wall to mechanical and hemodynamic stimuli[13]. It is usually the effect of a variety of complex pathophysiological mechanisms that are closely related, and that influences both the cellular and non-cellular components of the vascular wall. In the vascular system in fact morphology and functionality are closely related[11]. Altered flow conditions play an important role in the development of vein disease. In turn, all these flow conditions are modified by vein wall changes such as extrinsic stenosis or neoplastic infiltration.

One of the major hemodynamic stimuli is represented by the wall shear stress (WSS) that can be described as a tangential frictional force exerted by blood flow on the endoluminal surface of the

vessel wall[11,12]. The endothelial cells (ECs) respond to the modified WSS by determining an enlargement or a narrowing of vessel lumen in order to maintain WSS at a baseline level (0.8-2.0 Pa)[14]. If there is a prompt restitution of the WSS to baseline levels vascular remodelling is usually negligible with minimal intimal deposition of matrix fibers, myofibroblasts and smooth-muscle-cell[15]. If there is not a restitution to the normal WSS the balance between remodeling and destructive process of the vein can determine significant changes in the structure of the vessel involved[16].

The other hemodynamic force that can determine a vessel wall remodeling is the *tensile stress (TS)* (approximately 1000-2000 dynes $cm^{-1}$), a force normal to the vessel wall, which is equal to wall tension divided by the wall thickness[14]. Generally, vessel thickness changes proportionally to the wall tension in order to maintain TS at a baseline level[15,17,18]. Vessel enlargements and narrowings, or increase in portal pressure can determine important changes of the wall tension with associated modification of the TS. It is well known that patients with PDAC undergoing NCT can suffer from chemotherapy-associated liver injury that can determine an increase in liver stiffness and subsequently an increase in portal pressure with a modification of TS[19,20]. The development of portal hypertension (PH) in patients with pancreatic cancer can cause an increase in TS that can play a modulatory effect on portal remodelling that it is not well understood yet[21,22].

To date, little is known about the impact of degree of obstruction on the remodeling of portomesenteric vein wall. A useful method to estimate WSS is represented by computational fluid dynamics (CFD), which approximates the mathematical laws underlying the physical processes allowing to obtain quantitative results about blood velocity and pressure in patient-specific geometries[23-25]. Several factors need to be defined to perform the computational fluid dynamics analysis, including an accurate 3D geometry of the vein trunk created from imaging data and vein physiological parameters. Recently, a few works on CFD has been proposed to study blood dynamics in the human portal district where blood

dynamics changes have been studied in ideal geometries of the portal vein[22,23], and where real geometries of the portal district have been considered for the computational analysis[24-26]. A more complete computational model which accounts also for the liver perfusion has been proposed[27].

In this work we have investigated by means of CFD the hemodynamics and its potential effect on vascular remodeling in the portomesenteric trunk, with and without portal hypertension, in real models of patients with primitive and metastatic cancers of the pancreatic head, and different degrees of portal confluence obstruction. We have assessed the influence of WSS modifications on portal vein remodeling comparing hemodynamic data obtained from numerical simulations on real geometries to histopathologic findings of surgical specimens.

## METHODS

### Ethics Statement

This study was approved by the ethics committee and was performed in accordance with institutional ethics committee guidelines. All patients gave informed consent for the publication of their data.

### Clinical data, image acquisitions and reconstruction of computational geometries

We retrospectively enrolled in the study 6 patients referred to the General and Pancreatic Surgery Unit, Pancreas Institute, of the University of Verona with a diagnosis of borderline or locally advanced ductal adenocarcinoma or metastatic cancer of the pancreatic head who underwent radical surgery with some type of vein resection. Patients with diagnosis of borderline or locally advanced ductal adenocarcinoma of the pancreatic head of them underwent NCT with FOLFIRINOX (fluorouracil, leucovorin, oxaliplatin, and irinotecan) before surgery[6]. Patients with diagnosis of metastatic disease underwent upfront surgery. For each patient there was availability of preoperative contrast-enhanced CT scan and anatomopathological specimens.

Contrast-enhanced CT scan was performed by using two multislice equipment 64-detector rows (Briliance 64, Philips Healthcare, Best, The Netherlands; Perspective 64, Siemens Healthcare, Erlangen, Germany). Scans were acquired before and after 1.5 mL/kg intravenous injection of iodure contrast media (Ultravist 370, Schering, Berlin, Germany) during pancreatic arterial phase (15s after aortic bolus-tracking peak), venous phase (60-70s) and equilibrium phase (5 min). Section thickness was 2 mm, kv 120, and mAs 125-150. Parameters evaluated were: tumor volume and dimensions, tumor location, involvement of splanchnic vessels and presence of perivascular cuff.

For each patient a computational mesh of the portal system was created (Fig.1). In p5 we were able to reconstruct also the portal collateral circulation (portal cavernoma) arising from the Henle trunk and ending into the portal vein. We refer to this case as p5-mod. Surface models of the portal district boundary lumen were reconstructed with a level-set segmentation technique (VMTK http://www.vmtk.org). Such models were then converted into volumetric meshes composed by tetrahedra to be used in CFD simulations (Fig. 1). We performed a refinement study with respect to space discretization, by testing that the results on WSS remained the same, up to a tolerance of 2%, when reducing the mesh size of a factor 20%. Accordingly, we have considered a characteristic mesh size equal to 0.1 cm, corresponding to a number of tetrahedra equal to about about 680k for p1, 430k for p2, 690k for p3, 390k for p4, 680k for p5, and 800k for p6.

Computational Fluid Dynamics

Due to the constant-in-time flow rate in the portal district, we considered steady numerical simulations for blood dynamics performed by using the Finite Elements library LifeV (http://www.lifev.org). Blood was assumed Newtonian and incompressible, the flow laminar and the walls rigid. These assumptions are well accepted for our cases since the diameter of the vessels is greater than 0.6 cm and flow rate is moderate (see below)[28]. The blood density was set equal to 1.06 g/cm$^3$, whereas the viscosity to 0.035 Poise. As for the boundary conditions, we considered three inlet sections, that is the superior and inferior mesenteric veins and the splenic vein. For p5

solely, we have two further inlet sections, that is the trunk of Henle and the mesentery vessel. At these inlet sections, parabolic velocity profiles have been prescribed. These profiles featured a maximum value equal to 17 cm/s at the splenic vein and to 21 cm/s for the other inlets. Stress-free conditions were prescribed at the two outflow sections, that is the right and left portal veins, supposing similar resistances downstream the two portal branches. In order to study the blood dynamics in a portal hypertensive condition, we also run a simulation for each case with a decreased flow rate to account for the presence of the hypertension (maximum value equal to 16 cm/s at the splenic vein and to 17 cm/s for the other inlets). We used P1-P1 Finite Elements stabilized by means of the SUPG-PSPG technique[28,29].

Morphological evaluation

An expert pathologist subsequently evaluated on surgical specimens tumor dimensions, margin infiltration, presence and grade of vascular involvement/infiltration. All specimens were traditionally processed preparing formalin fixed-paraffin embedded (FFPE) samples. After this step, tissue blocks were cut obtaining 4 μm sections stained with hematoxylin-eosin for a conventional histological analysis. Evaluation of vascular wall structure and its modification was performed by further means of Masson's trichrome stain and immunohistochemical stain for smooth muscle actin (Alpha-Smooth Muscle Actin Monoclonal Antibody, 1A4, Agilent Dako, dilution 1:200).

## RESULTS

Five patients (p1, p2, p3, p4, p5) underwent total pancreatectomy (TP), one patient (p6) had duodenopancreatectomy (DP). Portal confluence or SMV resection was performed en-bloc together with the main specimen due to the presence of severe adhesions between the pancreatic isthmus and the portal confluence. The venous reconstruction was performed by a direct end-to-end anastomosis

after mobilization of the liver and pushing upwards the mesenteric root. The patency of venous reconstruction was controlled by at least one ultrasound postoperatively. Characteristics of the patients are described in Table 1.

In patients with absence or minimal stenosis (p1, p2, p3) the computational study of velocitiy fields showed a laminar, not disturbed flow with a gradual decrease of velocity magnitude from superior mesenteric vein to portal vein, especially in the left wall of the venous trunk. Generally, velocity magnitude was higher in zones of curvature of superior mesenteric and splenic veins, at the portal confluence and at the right wall immediately after the portal bifurcation, due to the flow coming from the splenic vein. In p2 a velocity peak was found at the portal bifurcation due to the angulation of the bifurcation. In the same cases with simulated portal hypertension analogous qualitative flow distribution was observed, but peak values were lower due to less flow rate entering the system. In patients with a critical stenosis (p4, p5, p6) the velocity magnitude was found to increase at the stenotic segment of the portal confluence, especially at different levels the left wall of the portomesenteric trunk with elevated peak values in each patient. Beyond the stenosis the portal vein appeared dilated and characterized by the presence of a chaotic and disturbed flow due to the presence of turbulent flow. Velocity streamlines for each patient are showed in Figure 2.

In patients with absence or minimal stenosis (p1, p2, p3) WSS magnitude showed near normal values (peak less than 1 Pa) with peak values near the portal bifurcation, with no evidence of negative or oscillatory WSS (Fig. 3). In patients with presence of critical stenosis (p4, p5 and p6) WSS magnitude showed high values (peak values > 1 Pa) in the stenotic segment at different levels of the portomesenteric trunk, especially near the confluence and in the left wall of the vessel, with elevated peak values in each patient. Wide areas of low WSS were found in the portal vein immediately after the stenosis, characterized also by negative and oscillatory values due to turbulent flow and areas of recirculation. Again, the presence of portal hypertension led to a slight decrease in the maximum WSS values. Figures 4 and 5 shows the different distribution of the WSS along the right and left port-mesenteric trunk in patients with and without stenosis. In P5 the presence of portal cavernoma

showed a more homogeneous distribution of WSS with near normal values in the whole system (fig.6). The computational simulation in the absence of portal cavernoma showed higher values of WSS at the portal stenosis with wide areas of disturbed flow and low WSS before the portal bifurcation.

The comparison of hemodynamic results to histopathological findings showed that in patients without a critical stenosis (e.g. in p2) and where no areas of high WSS were found, modifications of the vessel wall were only local and minimal, and mainly due to tumor infiltration, but the three-layered wall of the vessel was always preserved (Fig.7). In these patients ECs and the internal elastic lamina (IEL) were intact. The thickness of the vein wall was preserved with a normal wall-to-cavity ratio. In turn in patients with a critical stenosis (p4, p5, p6) areas with a high WSS corresponded to vessel regions characterized by severe wall derangements with an increase thickness of the tunica media and substitution of part of the vessel wall by fibrous tissue. In particular, in p4 (fig.8) the neoplastic growth is clearly visible forming an incomplete perivascular cuff with no infiltration of the vein. In p5 the three-layered structure of the resected vein was almost completely lost with complete derangement of the IEL in the segment exposed to high levels of WSS. In the same patient the vein wall was replaced by a dense inflammatory infiltrate with the almost completely disappearance of smooth muscle cells (SMC) (Fig. 9). The thickness of the vein wall was diminished with a reduced wall-to-cavity ratio. Also in p6 the three-layered structure of the resected vein was almost completely lost with severe derangement of the IEL in the segment exposed to high levels of WSS. In this patient the vein wall was replaced by a dense inflammatory infiltrate with subintimal migration of smooth muscle cells (SMC) (Fig. 10).

**DISCUSSION**

In this study we showed that modifications of the portal confluence in primitive and metastatic cancer of the pancreatic head elicit a wide spatiotemporal variation of WSS that modified the integrity of the vessel wall. In the portomesenteric trunk the presence of areas of high WSS aligned with the axial direction of flow due to critical stenoses caused severe derangement of the vein wall with

loss of the three-layered structure of the vessel wall. These areas of high WSS were followed by areas of low and oscillatory WSS, characterized by local vessel enlargement with severe intimal thickening and tunica media rearrangement. These modifications in local hemodynamics in fact triggered an endothelium-mediated response that usually regulates vessel caliber, structure[9,11,12] and remodeling[9,12,30]. Endothelial cells in fact act basically as sensors of WSS and by means of a complex mechanotransduction process that involves the whole vein wall maintain vascular homeostasis[31,32]. In response to hemodynamic solicitations, the endothelium synthetizes and secretes biologically active substances that control smooth-muscle-cell tone, vasal diameter and wall composition[12]. This adaptation has usually a trophic and protective effect on the vessel, preserving the original wall-to-lumen ratio even when a modification of the vessel size occurs[33]. There is however a threshold at which WSS switches from being a trophic and protective signal to having detrimental effects on ECs, resulting in mechanical damage to ECs surface integrity[11].

Basically, reduction of blood-flow velocity resulting in low WSS is considered a stimulus for intimal thickening with consequent lumen narrowing and normalization of WSS[10]. Intimal thickening, whether or not followed by rearrangement of the tunica media of the vein, usually occurs at the site of low or oscillating WSS and high particle residence time, such as the inlet side of branch ostia, on the opposite the flow divider in vascular bifurcations, or after a critical stenosis[14]. In turn, an increase in blood flow velocity resulting in a sustained elevation of WSS is a signal for a vessel enlargement until a restitution to the baseline WSS occurs and the vessel expansion stops[11,30,34]. The increase in luminal diameter is followed by relatively small changes in wall thickness, in order to compensate the increase in wall tension[14].

If a pathological elevation of WSS occurs as in critical stenoses, the outward remodeling process is characterized by increased luminal diameter with severe changes in wall thickness[34,35], derangement of the IEL[14,34,36] and proliferation of ECs and subintimal migration of SMCs[32, 36], as showed in patients of this series with critical stenosis. This outward remodeling is usually observed in vein bypass grafting and cerebral aneurysm remodeling where an impaired ECs response is the trigger for

the excessive wall degeneration with IEL and cell loss, SMCs migration and proliferation in the intima[16]. It has recently been demonstrated that matrix degradation and cell loss specifically occur in regions of accelerating flow, where WSS is high and WSS gradient is positive[16]. In turn, adjacent regions experiencing a decelerating flow, with a negative WSS gradient, remain generally undamaged, suggesting that the ECs respond differently to positive and negative WSS gradient[12]. In this environment a significant increase in the production of metalloproteinases (MMPs) with cell proliferation under arterial flow is observed[37-39], and the vessel wall changes in response to the new arterial environment and its associated shear stress, oxygen tension, metabolite concentrations, and pH[11,40]. Persistent pathological levels of high WSS along with the impossibility of the vessel to continue the outward remodeling as in cases of vein encasement by the tumor disrupt the balance between eutrophic remodeling and degradative process of the vein resulting in almost complete loss of its three-layered structure and its replacement with fibro-inflammatory tissue (see fig.9).

This last finding could have important consequences in surgical practice. In fact one of the paramount steps of PD is the dissection of the pancreatic neck from the SMV[41]. It is common experience that extensive wall infiltration by the tumor along with its desmoplastic reaction and fibrosis can make dissection hazardous and have a high risk of bleeding due to the absence of viable dissection plane between the pancreas and the portal confluence. In these cases a total pancreatectomy with en-bloc resection of the portal confluence is a reasonable option. Analogously, the preoperatory finding of a critical stenosis of the portal confluence, even without clear evidence of vein infiltration by the tumor, should compel surgeons to consider a possible TP. In fact in these cases the modifications of the vein can end up in the complete loss of the three-layered wall. In the absence of a three-layered structure repair of the vein, if damaged during surgical dissection, can be very difficult or impossible due to its extensive substitution by inflammatory and fibrous tissue. This study suggests that TP with en-bloc resection of the portal confluence could be the safest surgical approach in every case of critical stenosis of the portal confluence, avoiding any dissection of the pancreatic neck.

This computational study showed also that the simulation of an increase in portal pressure acted as a mitigating factor of high WSS consequences, reducing sensitively flow velocity and the resulting WSS. Cirrhotic patients with PH are known to be characterized by noticeable hemodynamic changes represented by low flow velocities and low levels of WSS[42]. Experimental studies have confirmed that the increase in hepatic resistance is followed by a reduction in flow velocities and WSS and accompanied by an increase in vessel stiffness due to deposition of ECM and migration of SMCs[21]. In this study we confirmed that PH has a protective effect on the WSS levels, lowering the magnitude of WSS on ECs in all the simulated cases, especially in zones of vessel narrowing. This condition has however conflicting effects on vein structure. Infact from one hand PH mitigates the effects of a high WSS on stenotic segments, on the other hand it reduces WSS in post-stenotic areas already characterized by low and oscillatory WSS. This reduction further impairs ECs that can show a proinflammatory phenotype with increased procoagulant and proadhesive properties[43,44], resulting in an increase risk of thrombotic events. This must be taken into account if a vessel resection is planned or if a iatrogenic injury occurs. This computational study indirectly confirms that the risk of vessel thrombosis is higher in patients with a portal cavernoma, as showed in the simulation in p5 (see fig.6). Infact the increase in the splanchnic vascular bed occurring in critical stenoses of the portal confluence is followed by a further reduction in WSS with worsening of ECs functions.

## CONCLUSIONS

A detailed understanding of the local hemodynamic environment, the influence of wall modifications due to modified flow patterns and the long-term adaptations of the vein to the new flow conditions wall can have useful surgical applications, especially in cases of involvement of portal confluence by the tumor growth. The comparison of computational data with histopathological findings showed that veins involved by neoplastic growth undergo a vascular remodelling that is not only due to a wall infiltration by the tumor but also to persistent pathological levels of WSS and TS that disrupt the balance between eutrophic remodeling and degradative process of the vein wall. Wall infiltration by the tumor, if not accompanied by critical stenosis, is usually followed by a vein remodeling that preserves the

three-layered wall of the vessel, even when the vessel wall is widely infiltrated. Modifications of local hemodynamics in a critical stenosis can lead to a complete substitution of the three-layered vein wall with disappearance of the dissection plane between pancreas and portal confluence compelling surgeons to conceive a different approach to pancreatic dissection in order to prevent injuries to the portal confluence.

**REFERENCES**


1. Chu LC, Goggins MG, Fishman EK. Diagnosis and Detection of Pancreatic Cancer. Cancer J 2017;23:333-342.
2. Isaji S, Mizuno S, Windsor JA, Bassi C, Fernández-Del Castillo C, Hackert T et al. International consensus on definition and criteria of borderline resectable pancreatic ductal adenocarcinoma 2017. Pancreatology 2018;18:2-11.
3. Delpero JR, Sauvanet A. Vascular resection for pancreatic cancer: 2019 French recommendation based on a literature review form 2008 to 6-2019. Front Oncol. 2020;10:40.
4. Tewari M. Significance of pathological positive superior mesenteric/portal venous invasion in pancreatic cancer. Hepatobiliary Pancreat Dis Int 2016;15:572-578.
5. Kaissis GA, Lohofer FK, Ziegelmayer S, Danner J, Jager C, Schirren R, et al. Borderline-resectable pancreatic adenocarcinoma: contour irregularity of the venous confluence in pre-operative computed tomography predicts histopathological infiltration. PLoS One. 2019;14(10): e0218642.
6. Maggino L, Malleo G, Marchegiani G, Viviani E, Nessi C, Ciprani D, et al. Outcomes of primary chemiotherapy for borderline resectable and locally advanced pancreatic ductal adenocarcinoma. JAMA Surg 2019, doi: 10.1001/jamasurg.2019.2277. [Epub ahead of print].
7. Li W. Biomechanical property and modelling of venous wall. Prog Biophys Mol Biol 2018;133:56-75
8. Korshunov VA[1], Berk BC. Flow-induced vascular remodeling in the mouse: a model for carotid intima-media thickening. Arterioscler Thromb Vasc Biol 2003;23:2185-2191.
9. Glagov S, Weisenberg E, Zarins CK, Stankunavicius R, Kolettis GJ. Compensatory enlargement of human atherosclerotic coronary arteries. N Engl J Med 1987;316:1371-1375.
10. Zarins CK, Zatina MA, Giddens DP, Ku DN, Glagov S. Shear stress regulation of artery lumen diameter in experimental atherogenesis. J Vasc Surg 1987;5:413-420.

11. Chiu JJ, Chien Shu. Effects of disturbed flow on vascular endothelium: pathophysiological basis and clinical perspectives. Physiol Rev 2011;91:327-387.
12. Dolan JM, Kolega J, Meng H. High wall shear stress and spatial gradients in vascular pathology: a review. Ann Biomed Eng 2013;41:1411-1427.
13. O'Rourke MF[1], Nichols WW. Aortic diameter, aortic stiffness, and wave reflection increase with age and isolated systolic hypertension. Hypertension 2005;45:652-658.
14. Quarteroni A , Tuveri M, Veneziani A. Computational vascular fluid dynamics: problems, models and methods. Comput Visual Sci 2000;2:163-197.
15. Langille B. Remodeling of developing and mature arteries: endothelium, smooth muscle and matrix. J Cardiovasc Pharmacol 1993;21:S11–S17.
16. Meng H, Tutino VM, Xiang J, Siddiqui A. High WSS or low WSS? Complex interactions of Hemodynamics with intracranial aneurysm initiation, growth and rupture: toward a unifying hypothesis. Am J Neuroradiol 2014;35:1254-1262.
17. N Masawa [1], S Glagov, C K Zarins. Quantitative morphologic study of intimal thickening at the human carotid bifurcation: II. The compensatory enlargement response and the role of the intima in tensile support. Atherosclerosis 1994;107:147-155.
18. Li W. Biomechanical property and modelling of venous wall. Prog Biophys Mol Biol 2018; 133:56-75.
19. Khan AZ, Morris-Stiff G, Makuuchi M. Patterns of chemotherapy-induced hepatic injury and their implications for patients undergoing liver resection for colorectal liver metastases. J Hepatobiliary Pancreat Surg 2009;16:137-144.
20. Viganò L, Rubbia-Brandt L, De Rosa G, Majno P, Langella S, Toso C, et al. Nodular regenerative hyperplasia in patients undergoing liver resection for colorectal metastases after chemotherapy: risk factors, preoperative assessment and clinical impact. Ann Surg Oncol 2015;22:4149-4157.

21. He XJ, Huang TZ, Wang PJ, Peng XC, Li WC, Wang J, et al. Morphological and biomechanical remodeling of the hepatic portal vein in a swine model of portal hypertension. Ann Vasc Surg 2012;26:259-267.
22. Hori N, Wiest R, Groszmann RJ. Enhanced release of nitric oxide in responde to changes in flow and shear stress in th superior mesenteric arteries of portal hypertensive rats. Hepatology 1998;28:1467-1473.
23. Perktold K, Resch M.1990. Numerical flow studies in human carotid artery bifurcations: basic discussion of the geometric factor in atherogenesis. J Biomed Eng 1990;12:111-123.
24. Taylor C, Figueroa C. Patient-specific modeling of cardiovascular mechanics. Annu Rev Biomed Eng 2009;11:109-134.
25. Quarteroni A, Dede' L, Manzoni A, Vergara C. Mathematical Modelling of the Human Cardiovascular System - Data, Numerical Approximation, Clinical Applications, Cambridge Monographs on Applied and Computational Mathematics, Cambridge University Press, 2019
26. Petkova S, Hossain A, Naser J, Palombo E. Cfd Modelling of Blood Flow in Portal Vein Hypertension With and Without Thrombosis, Third Int. Conf. CFD Miner. Process Ind., vol. 4, no. December, pp. 527–530, 2003.
27. Carvalho P. Analysis and Simulation of Blood Flow in the Portal Vein with Uncertainty Quantification. PhD thesis, Universidade Técnica de Lisboa, 2011.
28. George SM, Coulter W. Hemodynamic Investigation of the Liver Using Magnetic Resonance Imaging and Computational Fluid Dynamics. PhD thesis, Georgia Institute of Technology, 2008.
29. Tezduyar TE. Stabilized finite element formulations for incompressible flow computations. Adv Appl Mech 1991;28:1–44.
30. Gibbons GH, Dzau VJ. The emerging concept of vascular remodeling. N. Engl. J. Med. 1994;330:1431–1438.
31. Dolan JM, Meng H, Singh S, paluch R, Kolega J. High fluid shear stress and spatial shear stress gradients affect endothelial proliferation, survival and alignment. Ann Biomed Eng 2011;39:1620-1631.

32. Chien S. Effects of disturbed flow on endothelial cells. Ann Biomed Eng 2008;36:554-562

33. Mulvany MJ, Baumbach GL, Aalkjaer C, Heagerty AM, Korsgaard N, Schiffrin EL, et al. Vascular remodeling. Hypertension 1996;28:505-506.

34. Tronc F, Mallat Z, Lehoux S, Wassef M, Esposito B, Tedgui A. Role of matrix metalloproteinases in blood flow-induced arterial enlargement: interaction with NO. Arterioscler Thromb Vasc Biol 2000;20:E120–E126.

35. Lehman RM, Owens GK, Kassell NF, Hongo K. Mechanism of enlargement of major cerebral collateral arteries in rabbits. Stroke. 1991;22:499–504.

36. Masuda H, Zhuang YJ, Singh TM, Kawamura K, Murakami M, Zarins CK, et al. Adaptive remodeling of internal elastic lamina and endothelial lining during flow-induced arterial enlargement. Arterioscler Thromb Vasc Biol 1999;19:2298–2307.

37. Sho E, Sho M, Singh TM, Nanjo H, Komatsu M, Xu C, et al. Arterial enlargement in response to high flow requires early expression of matrix metalloproteinases to degrade extracellular matrix. Exp Mol Pathol 2002;73:142–153.

38. El-Omar M, Dangas G, Iakovou I, Mehran R. Update on in-stent restenosis. Curr Interv Cardiol Rep. 2001;3:296–305.

39. Mavromatis K, Fukai T, Tate M, Chesler N, Ku DN, Galis ZS. Early effects of arterial hemodynamic conditions on human saphenous veins perfused ex vivo. Arterioscler Thromb Vasc Biol. 2000;20:1889–1895.

40. Davies MG, Hagen PO. Pathophysiology of vein graft failure: a review. Eur J Vasc Endovasc Surg. 1995;9:7–18.

41. Christians KK, Evans DB, Pedrazzoli S, Sperti C, Beaulieu R, Eckhauser F, et al. Resection for neoplasms of the pancreas. Clavien P-A, Sarr MG, Fong Y, Miyasaki M (Eds). Atlas of Upper Gastrointestinal and Hepato-Pancreato-Biliary Surgery. 2nd Ed, Berlin-Heidelberg, Springer-Verlag, 2016, 831-872.

42. Cichoz-Lach H, Celinski K, Slomka M, Ksztelan-Szczerbinska B. Pathophysiology of portal hypertension. J Physiol Pharmacol 2008;59(suppl.2):231-238.

43. Li X, Wang XK, Chen B, Pu YS, Li ZF, Nie P, et al. Computational hemodynamics of portal vein hypertension in hepatic cirrhosis patients. Biomed Mater Eng 2015;26:S233–S243.
44. Wei W, Pu YS, Wang XK , Jiang A, Zhou R, Li Y, et al. Wall shear stress in portal vein of cirrhotic patients with portal hypertension. World J Gastroenterol 2017;23:3279–3286.

LEGENDS

Fig.1. Computational meshes composed by tetrahedra generated for each case starting from the CT images and used for the numerical simulations.

Fig.2. The figure shows a laminar, not disturbed flow with a gradual decrease of velocity magnitude from superior mesenteric vein to portal vein, especially in the left wall of the venous trunk in patients without stenosis (P1, P2 and p3). In patients with a critical stenosis (p4, p5 and p6) the velocity magnitude was found to increase at the stenotic segment of the portal confluence, especially at different levels the left wall of the portomesenteric trunk with elevated peak values in each patient. Beyond the stenosis a large area of flow separation is visible and complex helical flow patterns occupy the separated flow region.

Fig.3. The figure shows the WSS distribution in each patient. In patients with absence or minimal stenosis (p1, p2, p3) WSS magnitude was homogeneously distributed and showed near normal values (peak less than 1 Pa) with no evidence of negative or oscillatory WSS. In patients with presence of critical stenosis (p4, p5 and p6) WSS magnitude showed high values (peak values > 1 Pa) in stenotic segments, especially near the confluence and in the left wall of the vessel. In these patients wide areas of low WSS were found in the portal vein immediately after the stenosis, characterized by negative and oscillatory values due to turbulent flow and areas of recirculation. In P6 the presence of portal cavernoma showed a more homogeneous distribution of WSS with near normal values in the whole system.

Flg.4. Wall shear stress along the axis of the portomesenteric trunk on both sides of the siymmetry plane in patients without stenosis.

Fig.5. Wall shear stress along the axis of the portomesenteric trunk on both sides of the siymmetry plane in patients with critical stenosis.

Fig.6. The figure shows the behavior of the WSS in the portomesenteric trunk in p5 with and without portal cavernoma. The hemodynamic simulation in the presence of the neoformed portal circulation showed a homogeneous distribution of the velocity field and the resulting WSS at the portal confluence. In the absence of portal cavernoma pathological values of WSS were found especially at the level of portal confluence.

Fig. 7. A: particular of normal portal confluence in p2. B: Histological appearance of a vascular structure infiltrated by adenocarcinomatous glands. Vascular wall is infiltrated by adenocarcinomatous glands (black arrow) with its desmoplastic reaction. Fibrosis (asterisk) accompanies adenocarcinomatous glands. C: Fibrosis (asterisk) involves, destructures and widens muscle fibers of the tunica muscularis nearby (white arrow). C: smooth-muscle actin, D: Masson's trichrome stain. Original magnification: 0.8x/2x.

Fig. 8. A: Total pancreatectomy with en-bloc resection of the portal confluence in p4 (black arrow). B: particular of the stenosis of the portal confluence (black arrow). C: Histological appearance of adenocarcinomatous glands (black arrow) lapping the portal confluence (white arrow: tumor front). Red arrows shows the thickened tunica media. D: The wall facing adenocarcinomatous glands (black arrows) appears thick and fibrotic (asterisk), the wall underneath appears thin, destructured with loss of muscle fibers (red arrow). C: smooth-muscle actin, D: Masson's trichrome stain. Original magnification: 1x/2x.

Fig. 9. A: particular of the stenosis of the portal confluence seen from behind in p5. B: Histological appearance of a pathologic vein's wall. The wall is thickened with prevalence of fibrosis (asterisk) and with destructured muscle fibers due to interspersed fibrosis (black arrow). C: the picture shows the

almost total disappearance of the three-layered vein wall with prevalence of fibrosis (asterisk) and with destructured muscle fibers due to interspersed fibrosis (black arrow). B: smooth-muscle actin, C: Masson's trichrome stain. Original magnification: 1.1x/2x. SV: splenic vein, IMV: inferior mesenteric vein, PV: portal vein, SMV: superior mesenteric vein, PC: portal cavernoma.

Fig. 10. A: particular of the stenosis of the portal confluence in p6 (black arrow). B: Histological appearance of a pathologic vein's wall. The wall is modified, thickened especially where massive fibrosis (asterisks) destructures and widens muscle fibers of the tunica muscolaris (black arrow). C: The figure shows the modified vein wall with massive fibrosis (asterisks) and thickened tunica muscularis (black arrows. B: smooth-muscle actin, C: Masson's trichrome stain. Original magnification: 1.1x/2x.

Figure 1

Click here to download Figure Fig1.tif

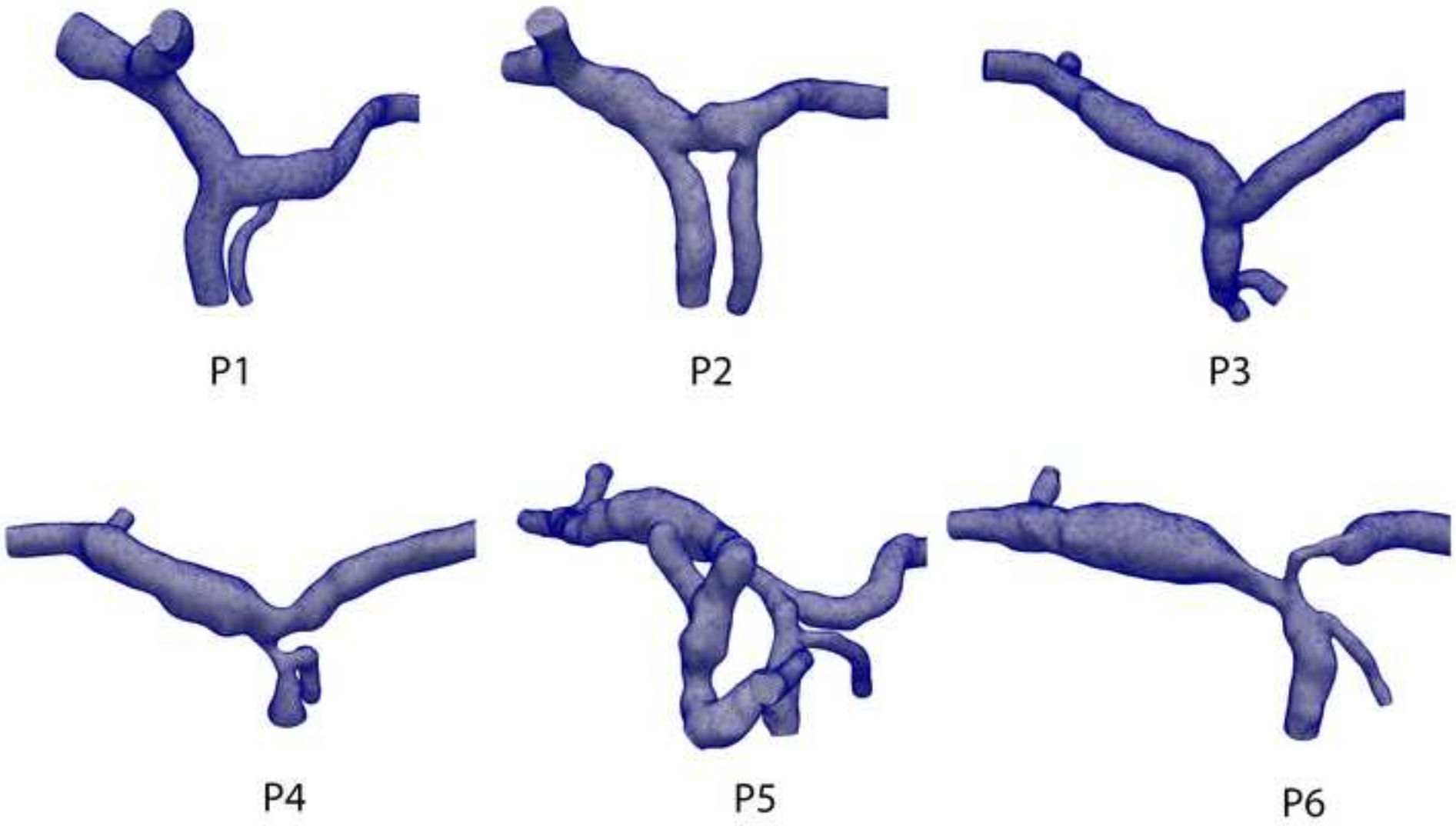

Figure 2

Click here to download Figure Fig2.tif

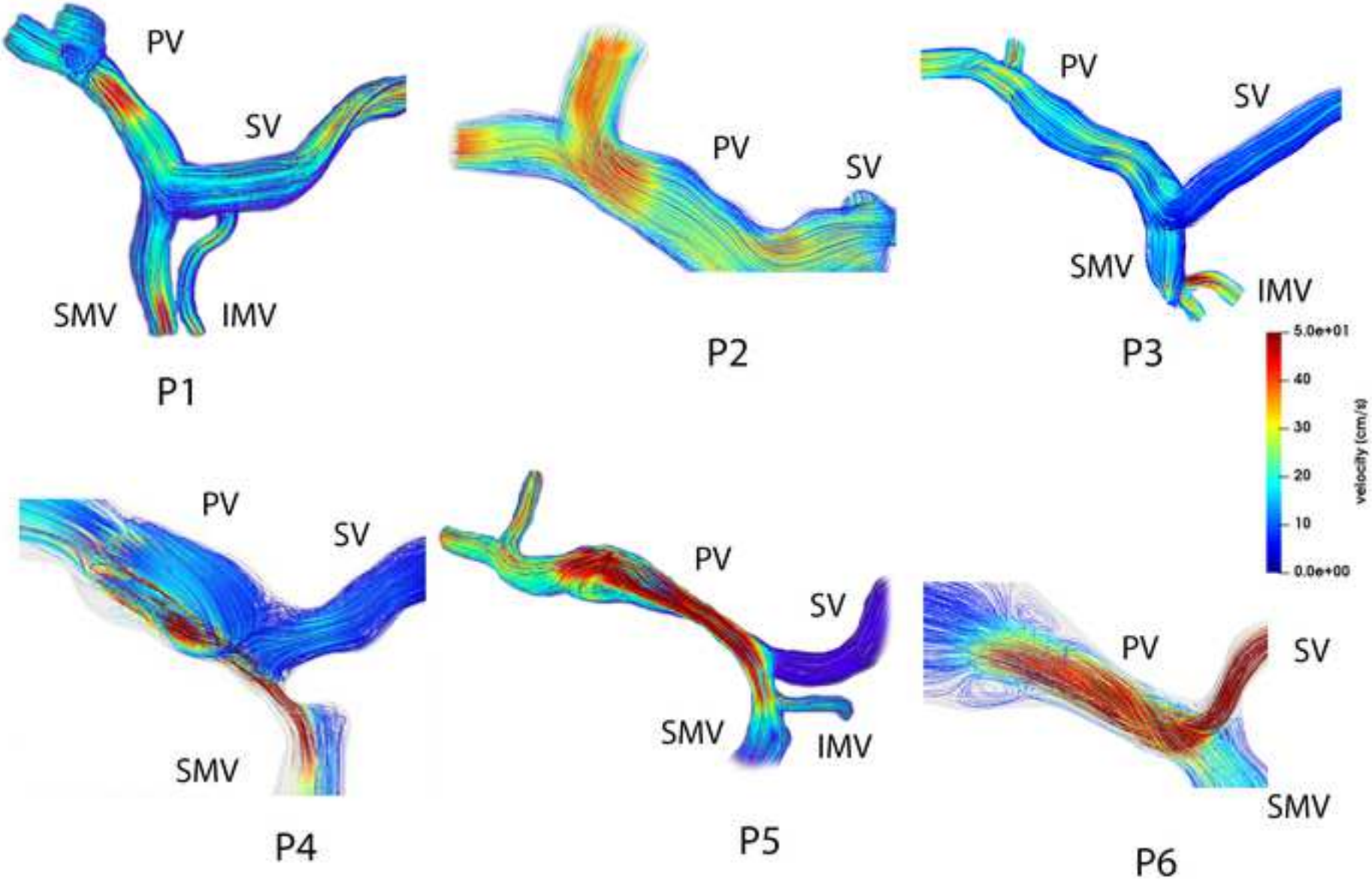

Figure 3

Click here to download Figure Fig3.tif

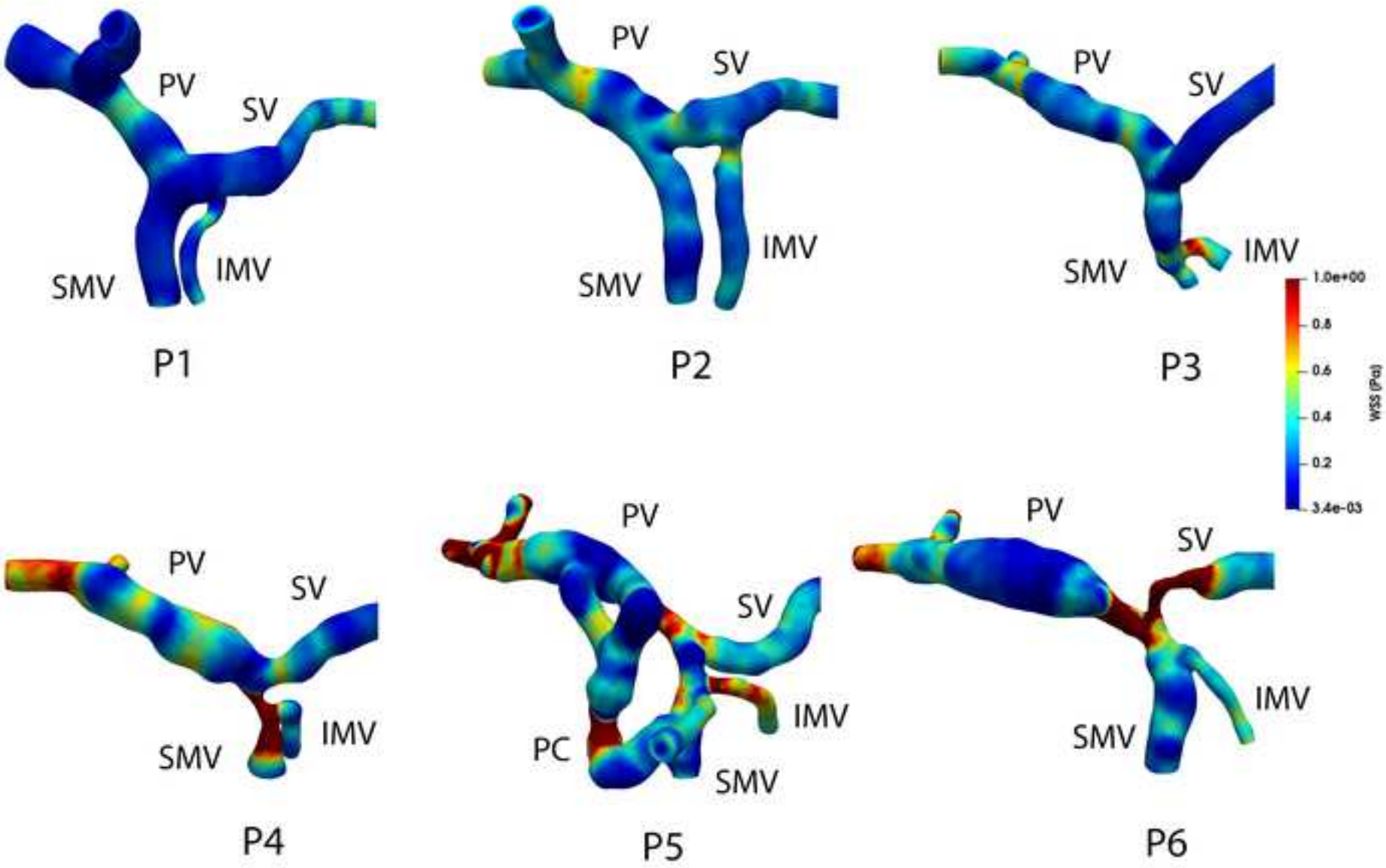

Figure 4

Click here to download Figure Fig4.tif

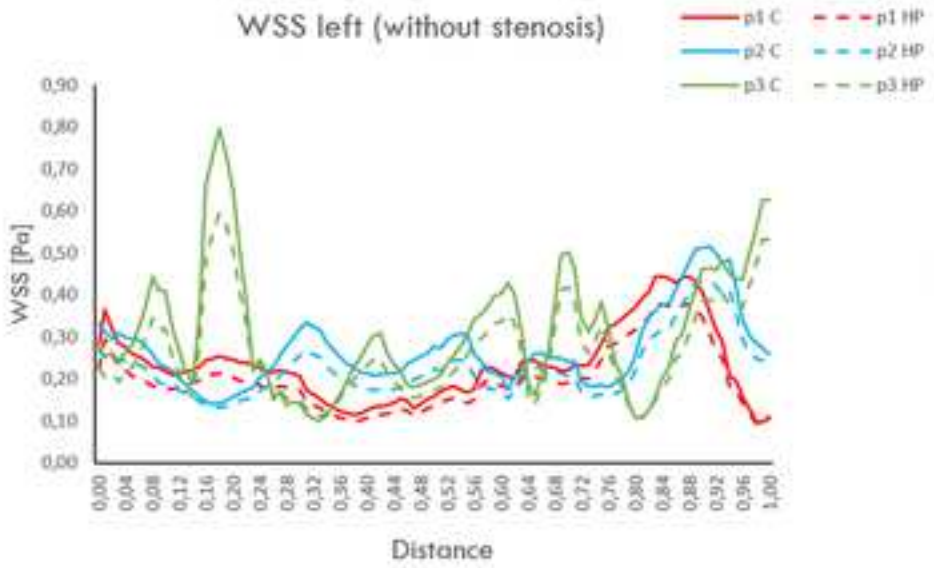


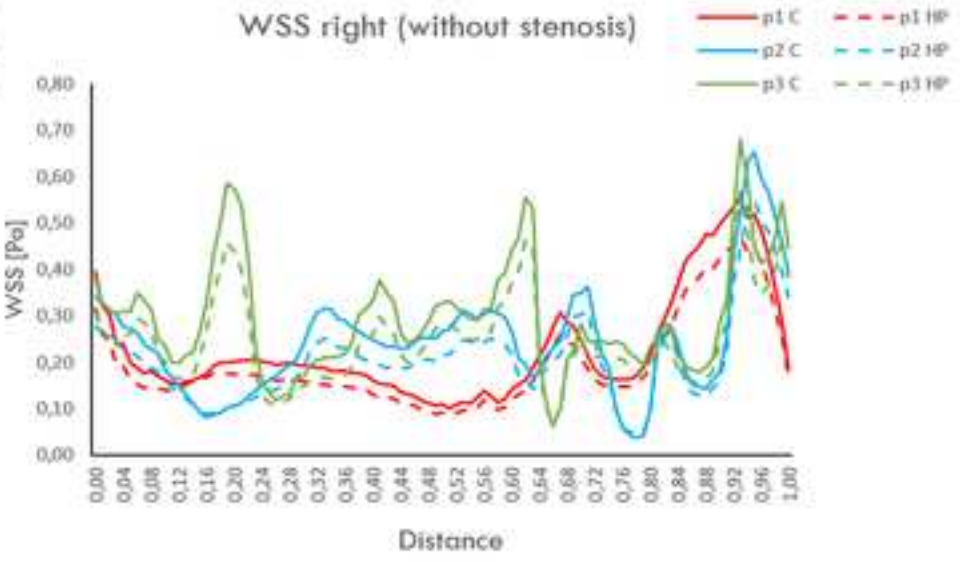

Figure 5

Click here to download Figure Fig5.tif

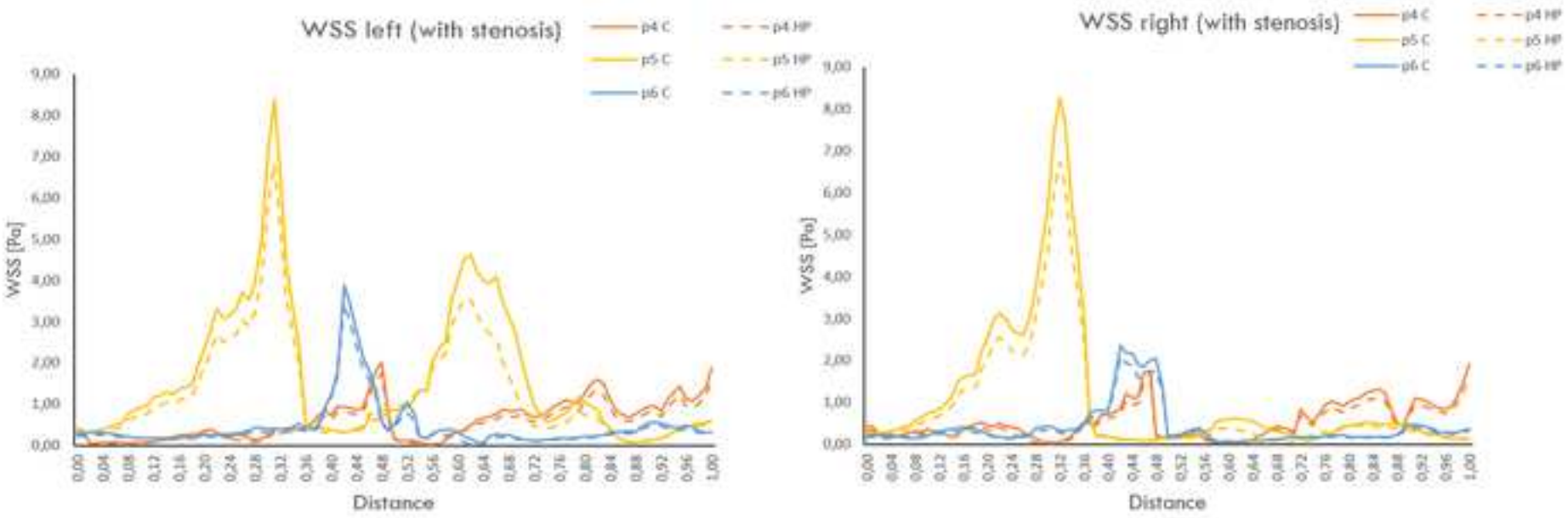

Figure 6

Click here to download Figure Fig6.tif

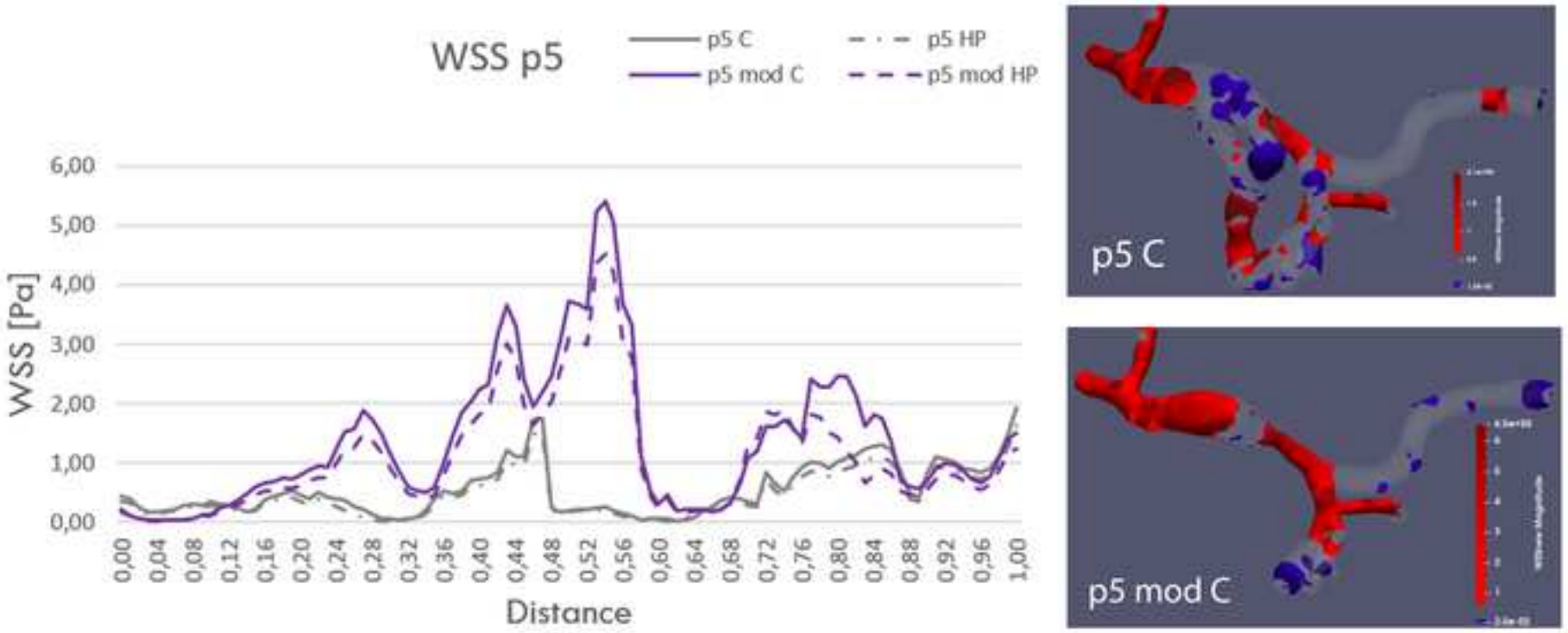

Figure 7

Click here to download Figure Fig7.tif

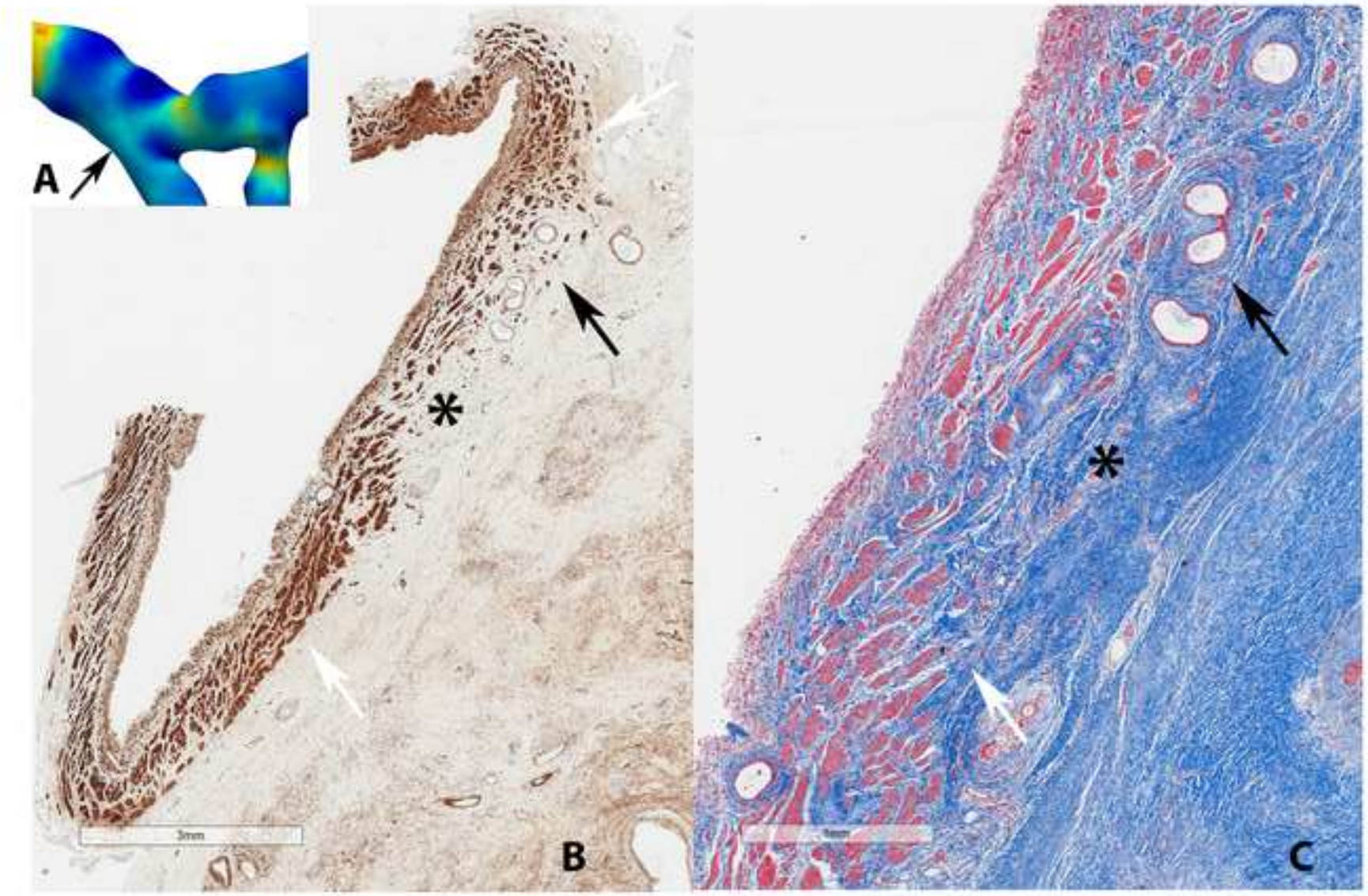

Figure 8

Click here to download Figure Fig8.tif

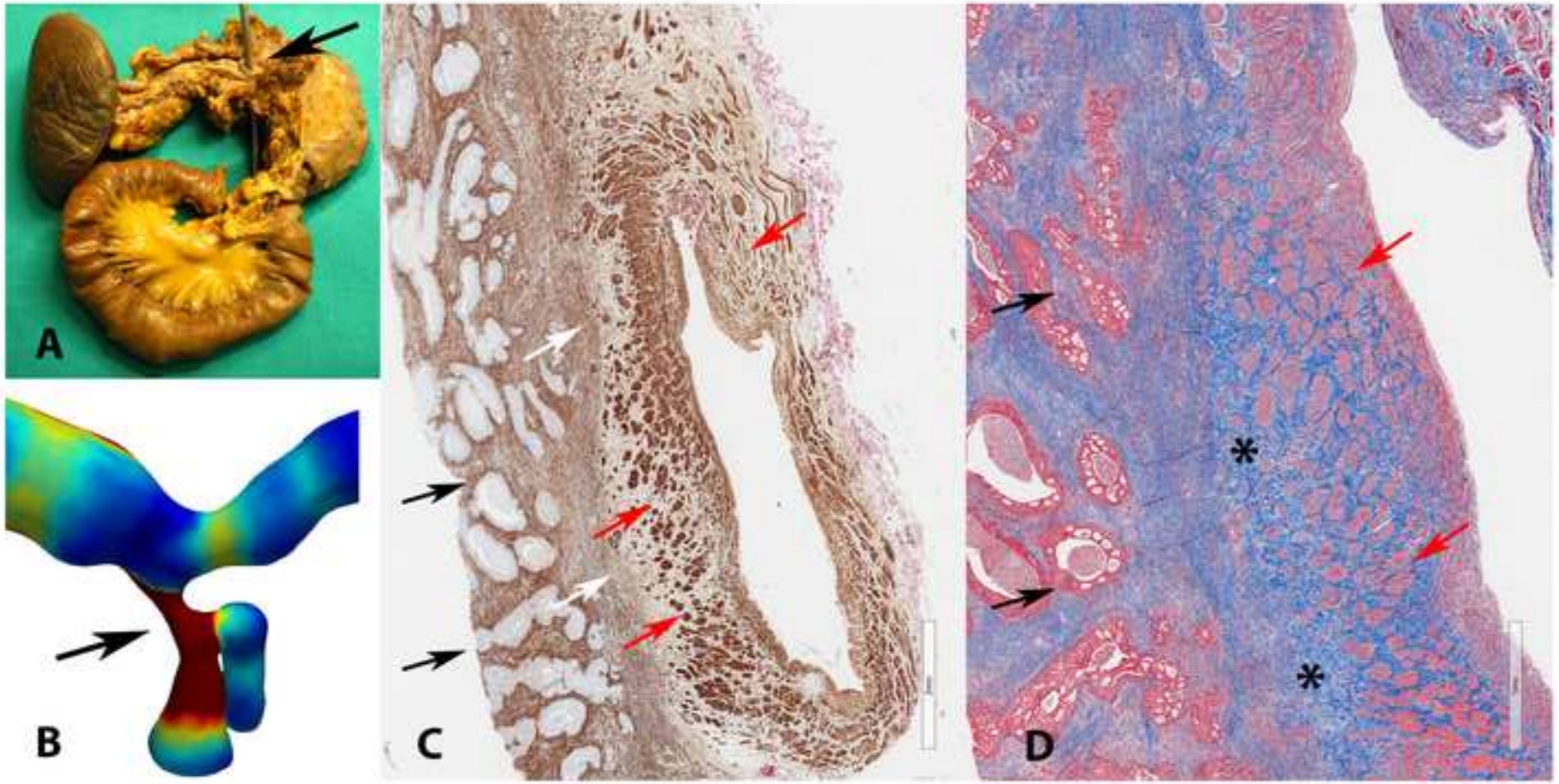

Figure 9

Click here to download Figure Fig9.tif

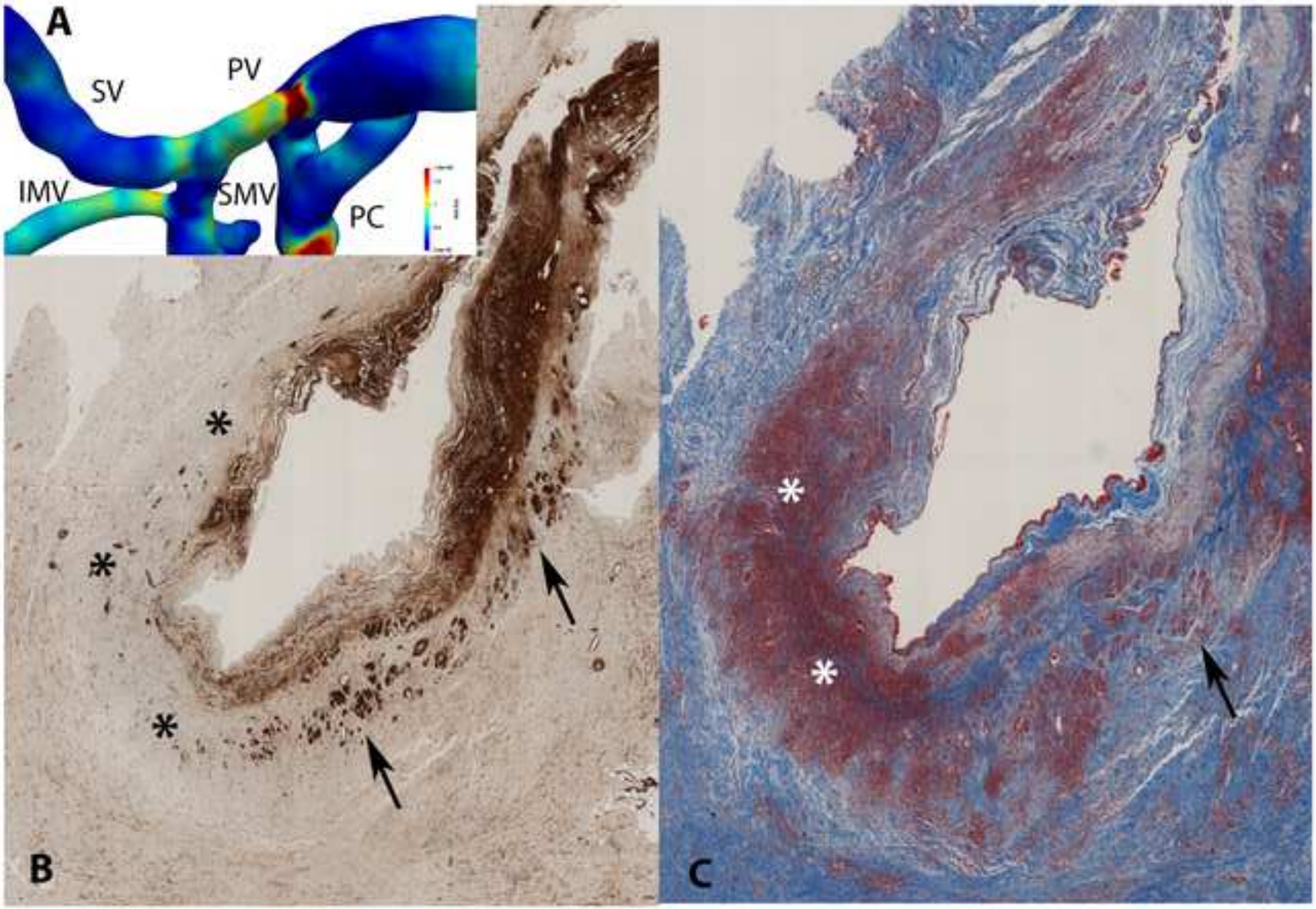

Figure 10

Click here to download Figure Fig10.tif

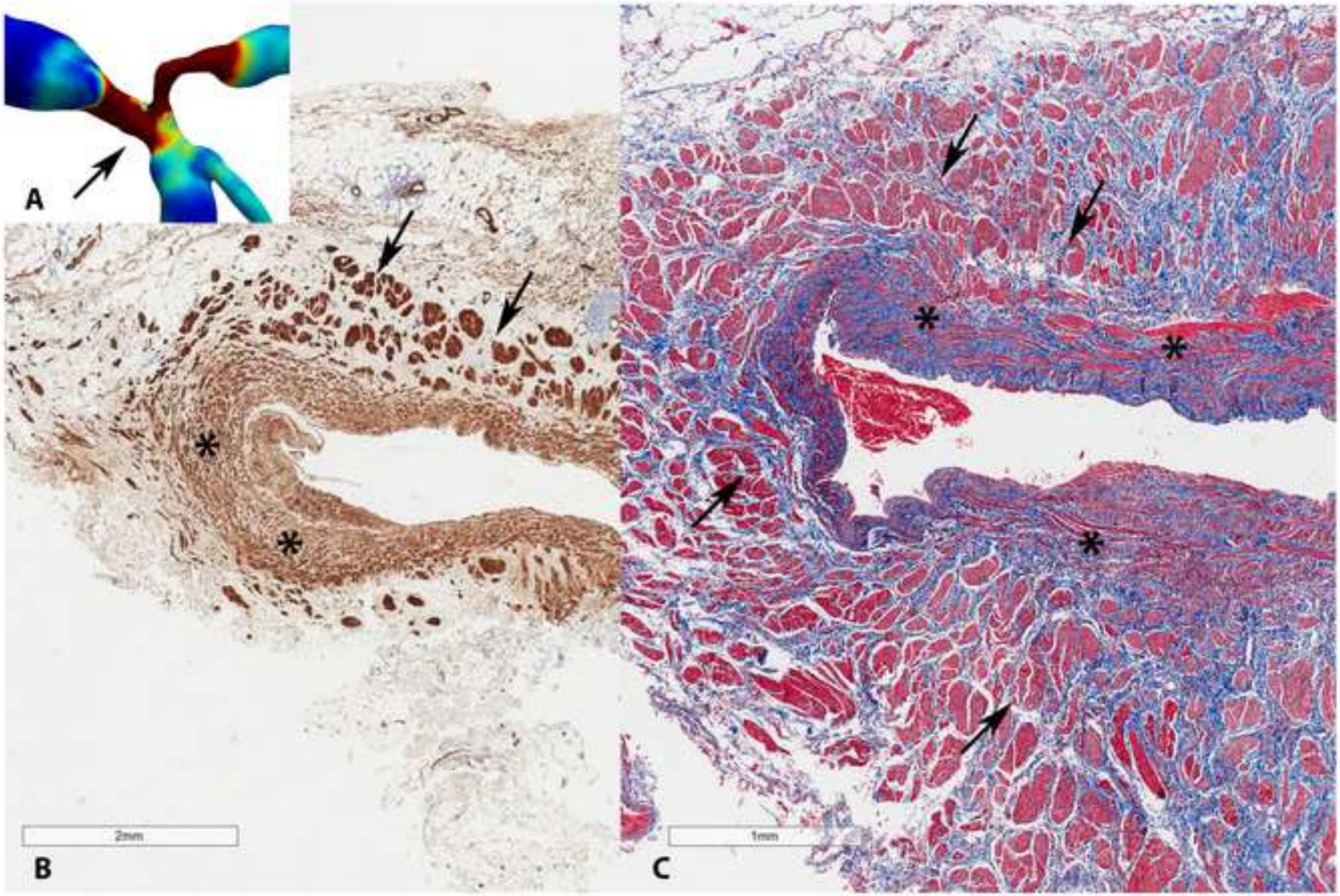

Table 1. Characteristics of patients.

| patient | age (sex) | CT findings | stenosis (%) | NCT (#) | RT | surgery | diagnosis | vascular involvement |
|---|---|---|---|---|---|---|---|---|
| 1 | 74 (M) | BR <180° | 10 | Folfirinox (10) | SBRT | TP EBR | adenocarcinoma with squamous features | full thickness intramural infiltration and discharge of neoplastic cells into the lumen |
| 2 | 68 (F) | BR <180° | 20 | Folfirinox (7) | SBRT | TP EBR | adenocarcinoma | focal intramural infiltration |
| 3 | 74 (M) | BR >180° | 10 | Folfirinox (14) | SBRT | TP EBR | carcinoma with solid growth pattern | focally full thickness, intramural infiltration |
| 4 | 55 (F) | BR <180° | 80 | none | none | TP EBR | metastasis (lung carcinoma) | absence of neoplastic infiltration, fibrous-inflammatory adhesion |
| 5 | 58 (F) | BR >180° | 90 | Folfirinox (12) | SBRT | TP EBR | adenocarcinoma with marked tumor regression | wall fibrosis, absence of neoplastic infiltration |
| 6 | 67 (M) | LA <180° | 80 | none | none | PD EBR | metastasis (colonic adenocarcinoma) | infiltration of the tunica adventitia |

NCT: neoadjuvant chemotherapy; RT: radiotherapy; SBRT: Stereotactic Body Radiation Therapy; BR: borderline resectable; TP: total pancreatectomy; PD: pancreatoduodenectomy; EBR: en-bloc resection;

Table 2. Hemodynamic parameters in patients with and without portal confluence stenosis and simulated portal hypertension.

| Parameters | velocity | | | WSS | | |
|---|---|---|---|---|---|---|
| | mean | max | min | mean | max | min |
| Patient 1 | | | | | | |
| without PH | 7.543 | 20.841 | 0.006 | 0.178 | 0.165 | 0.008 |
| with PH | 6.663 | 18.598 | 0.108 | 0.154 | 0.520 | 0.007 |
| Patient 2 | | | | | | |
| without PH | 9.345 | 22.214 | 0.194 | 0.318 | 0.752 | 0.007 |
| with PH | 8.138 | 19.129 | 0.139 | 0.273 | 0.632 | 0.004 |
| Patient 3 | | | | | | |
| without PH | 9.414 | 35.922 | 0.156 | 0.273 | 1.257 | 0.009 |
| with PH | 7.440 | 28.172 | 0.404 | 0.236 | 0.979 | 0.009 |
| Patient 4 | | | | | | |
| without PH | 16.221 | 214.46 | 0.150 | 0.595 | 9.408 | 0.013 |
| with PH | 13.272 | 174.39 | 0.211 | 0.483 | 7.654 | 0.011 |
| Patient 5 | | | | | | |
| without PH | 14.647 | 67.505 | 0.038 | 0.573 | 2.345 | 0.012 |
| with PH | 12.544 | 57.279 | 0.082 | 0.487 | 2.038 | 0.003 |
| Patient 6 | | | | | | |
| without PH | 11.268 | 193.06 | 0.094 | 0.487 | 3.983 | 0.003 |
| with PH | 10.079 | 181.81 | 0.087 | 0.424 | 3.578 | 0.012 |

WSS: wall shear stress; PH: portal hypertension.

# MOX Technical Reports, last issues

Dipartimento di Matematica
Politecnico di Milano, Via Bonardi 9 - 20133 Milano (Italy)

**62/2020** Massi, M. C.; Ieva, F.
*Representation Learning Methods for EEG Cross-Subject Channel Selection and Trial Classification*

**61/2020** Pozzi, S.; Redaelli, A.; Vergara, C.; Votta, E.; Zunino, P.
*Mathematical and numerical modeling of atherosclerotic plaque progression based on fluid-structure interaction*

**60/2020** Lupo Pasini, M; Perotto, S.
*Hierarchical model reduction driven by a Proper Orthogonal Decomposition for parametrized advection-diffusion-reaction problems*

**59/2020** Massi, M.C.; Franco, N.R; Ieva, F.; Manzoni, A.; Paganoni, A.M.; Zunino, P.
*High-Order Interaction Learning via Targeted Pattern Search*

**58/2020** Beraha, M.; Pegoraro, M.; Peli, R.; Guglielmi, A
*Spatially dependent mixture models via the Logistic Multivariate CAR prior*

**57/2020** Regazzoni, F.; Quarteroni, A.
*An oscillation-free fully partitioned scheme for the numerical modeling of cardiac active mechanics*

**56/2020** Botti, L.; Botti, M.; Di Pietro, D. A.;
*A Hybrid High-Order method for multiple-network poroelasticity*

**55/2020** Botti, M.; Castanon Quiroz, D.; Di Pietro, D.A.; Harnist, A.
*A Hybrid High-Order method for creeping flows of non-Newtonian fluids*

**54/2020** Arnone, E.; Bernardi, M. S.; Sangalli, L. M.; Secchi, P.
*Analysis of Telecom Italia mobile phone data by space-time regression with differential regularization*

**53/2020** Arnone, E.; Kneip, A.; Nobile, F.; Sangalli, L. M.
*Some numerical test on the convergence rates of regression with differential regularization*